

Supporting Information (SI) for Energy & Environmental Science.

Breathing air into water: dual-pathway H₂O₂ synthesis via aerating amphiphilic supramolecular films

Bo Yu,^a Shuya Liu,^{*b} Xinyu Lin,^a Zhi Zhu,^a Yongsheng Yan,^a Yanjun Gong,^c Yanke Che,^c Yan Yan,^{*a} and Weidong Shi^{*a}.

^a School of Chemistry and Chemical Engineering, Jiangsu University, Zhenjiang, 212013, China.

^b Institute of Resources and Environment Innovation, Shandong Jianzhu University, Jinan, 250101, China.

^c Key Laboratory of Photochemistry CAS Research/Education Center for Excellence in Molecular Sciences, Institute of Chemistry Chinese Academy of Sciences Beijing, 100190, China.

*Corresponding authors: Shuya Liu, Yan Yan, Weidong Shi

Email: liushuya@sdjzu.edu.cn; dgy5212004@163.com; swd1978@ujv.edu.cn

Experimental section.

1.1 Materials

Perylene-3, 4, 9, 10-tetracarboxylic dianhydride ($\geq 92.0\%$), imidazole (99%), sulfuric acid (H_2SO_4 , 98%), hydrochloric acid (HCl , 37%), 30% hydrogen peroxide (H_2O_2) stock solution, ethanol (EtOH , AR), methanol (MeOH , AR), tetrahydrofuran (THF), trichloromethane (CHCl_3 , $>99.9\%$, Extra Dry), catalase and p-benzoquinone (p-BQ) were obtained from Shanghai Aladdin Biochemical Technology Co. Anhydrous dichloromethane (DCM, $>99.9\%$, Extra Dry) was purchased from Energy Chemical Reagent Co., Ltd. Heavy oxygen water (H_2^{18}O , 97 atom % ^{18}O) was obtained from Sigma-Aldrich Company Ltd. China. All solvents and reagents obtained from commercial sources were used without further purification.

1.2. Synthesis of PDIOH

1.2.1 Synthesis of 1-(4-(aminomethyl)phenyl)propan-1-ol (A)

1.0 g of 2-(4-propionylphenyl) acetonitrile was mixed with 0.74 g of LiAlH_4 in THF, and then the mixture was stirred at 0°C under an argon atmosphere for 8 h. The reaction mixture was slowly quenched with a saturated ammonium chloride solution. The suspension was extracted with methylene chloride ($3 \times 50\text{ mL}$) and washed with salt water ($3 \times 10\text{ mL}$). The combined organic layer was dried on anhydrous sodium sulfate, filtered, concentrated under reduced pressure and purified on silica gel by column chromatography with 30:1 volume ratio of petroleum ether-acetate solvent system. Finally, the compound **A** was obtained.

1.2.2 Synthesis of 9-dodecyl-1H-isochromeno[6',5',4':10,5,6]anthra[2,1,9-def]isoquinoline-1,3,8,10(9H)-tetraone (B).

A mixture of 0.2 g of perylene-3,4,9,10-tetracarboxylic dianhydride and 1.0 g of dodecyl amine in 30 mL methanol conical flask was refluxed for 7 h. The resulting solid product was then cooled to room temperature and acidified with concentrated HCl (20 mL). After stirring overnight, the red solid was collected by vacuum filtration through a $0.45\text{ }\mu\text{m}$ membrane filter. The resulting mixture was centrifuged and washed with ethanol and deionized water until the solution was neutral ($\text{pH}=7$). Obtained compound **B** was collected and dried at 60°C in the vacuum for subsequent reactions.

1.2.3 Synthesis of PDIOH (C)

A mixture containing compound **A** (30 mg), compound **B** (20 mg), and imidazole (3 g) was heated to 140°C and stirred for 3 h under an argon atmosphere. The reaction mixture was then cooled to room temperature and dispersed in ethanol (25 mL), followed by the addition of concentrated HCl (20 mL). After stirring overnight, the

resulting red solid was collected by vacuum filtration through a 0.45 μm membrane filter and thoroughly washed with ethanol and distilled water. Finally obtained compound **C** (**PDIOH**) with amphiphilic groups. The resulting target compound was confirmed by ^1H NMR (**Fig. S4**).

1.3. Self-assembly of PDIOH fibers.

In a typical preparation procedure, 0.5 mg **PDIOH** precursor was dissolved uniformly in 5 mL of CHCl_3 (good solvent), then 5 mL ethanol (poor solvent) was added. The mixed solution was transferred into a 10 mL vial. Then the vials were sealed and placed on a 30°C hot stage for 24 h. The self-assembly sample was centrifuged and washed with water and dried until constant weight.

1.4. Self-assembly of PDIOH film

Typically, 100 μL of freshly prepared **PDIOH** chloroform solution (0.1 mg/mL) was slowly added to 10 mL of water in a 20 mL volumetric flask under draught cupboard ambient conditions. With slow evaporation of chloroform, the chloroform/water interface keeps shrinking. After 3 hours, all the chloroform has evaporated, a most highly ordered nanofiber film was left on the water surface, which call the 2D primary film (**M0**). By adjusting the amount of **PDIOH** chloroform solution (120 μL , 150 μL , 200 μL , and 250 μL), the secondary structure on the monolayer nanofiber membrane were gradually formed, which called **M1**, **M2**, **M3**, and **M4** in turn. Using this simple and low-cost method, we successfully fabricated Janus **PDIOH** film with gradient infiltration and fabricated them into photocatalysts with good photoresponse and stability.

1.5. Characterizations.

X ray diffractometer spectra were obtained via the X ray diffractometer (XRD, D8 Advance, Bruker) with $\text{Cu-K}\alpha$ radiation and the scanning step was 1°/min. The morphology of the samples was determined using scanning electron microscopy (SEM, Zeiss 300 Sigma) and transmission electron microscopy (TEM, FEL Tecnai G2 F20). The infrared spectra were obtained via Fourier infrared spectrometer (FT-IR, VERTEX-70, Bruker). UV–vis spectrophotometer (UV-vis DRS, U-3900, Hitachi) was employed to obtain both UV–vis absorption spectra. Confocal laser scanning microscopy (CLSM, LSM 880, ZEISS) was employed to observe the images of the sample at different depth levels. The colorimetric method was used to quantitatively detect H_2O_2 on a UV-vis spectrophotometer (UV-2450, Shimadzu, Japan). The isotopically labeled experiments were carried out on a gas chromatography-mass spectrometry (GC-MS, Agilent 7890B-5977B).

1.6. Photocatalytic H_2O_2 production.

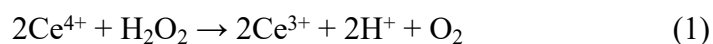
H_2O_2 was photocatalyzed by **PDIOH** film catalyst (0.03 mg) floated in a 10 mL deionized water glass reaction cell. Before the photocatalytic test, stand for 30 min to achieve the absorption and desorption equilibrium. Then,

Xenon lamp (Perfect PLS-SEX 300D) was used as a light source (optical density: $1000 \text{ mW} \cdot \text{cm}^{-2}$). During the reaction process, the temperature of the reaction system was kept stable (8°C) by the condensate system. Finally, the concentration of H_2O_2 was determined by UV-vis spectrophotometer.

Furthermore, to investigate the effects of scale, we expanded the experiment by significantly increasing the number of **PDIOH** films processed. Specifically, instead of the previous setup, we floated a larger quantity of films within the same 20 mL volume of deionized water, necessitating the use of a larger 50 mL container to accommodate the increased substrate loading while maintaining the liquid volume. All other reaction parameters remained strictly unchanged.

1.7. Determination of H_2O_2 concentration.

1.7.1. Cerous sulfate colorimetry. The concentration of H_2O_2 is determined by cerium $\text{Ce}(\text{SO}_4)_2$ titration based on the mechanism of reducing the yellow solution of Ce^{4+} to colorless Ce^{3+} through H_2O_2 (Equation (1)). The concentration of Ce^{4+} before and after the reaction was measured by UV-vis spectrophotometer. The absorption peak was 316 nm. The reaction formula is as follows:



$$M = 1/2 M\text{Ce}^{4+} \quad (2)$$

33.2 mg $\text{Ce}(\text{SO}_4)_2$ was dissolved in 100 mL 0.5 M sulfuric acid solution to prepare a yellow transparent $\text{Ce}(\text{SO}_4)_2$ solution (1.0 mM). The known concentration of H_2O_2 was added to the $\text{Ce}(\text{SO}_4)_2$ solution. According to the linear relationship between the signal strength and the concentration of Ce^{4+} , The hydrogen peroxide concentration of the sample can be obtained by using the UV-visible spectrophotometer to measure and obtain the standard curve. H_2O_2 concentration calculation formula (equation (2)).

1.7.2. Titanium sulfate colorimetry. 1 mL $0.1 \text{ mol} \cdot \text{L}^{-1}$ titanium sulfate ($\text{Ti}(\text{SO}_4)_2$) aqueous solution and 1 mL $0.1 \text{ mol} \cdot \text{L}^{-1}$ sulfuric acid aqueous solution were added to the obtained solution, which was then kept for 1 h. H_2O_2 molecules react with titanium sulfate under acidic conditions to form titanium complexes (with strong absorption near 416 nm). The absorbance of titanium complexes at 416 nm is measured by UV-visible spectrophotometer, and then the amount of H_2O_2 generated by each reaction can be calculated.

1.8. AQY measurements

The photocatalytic reaction was carried out in pure deionized water (20 mL) and catalyst (0.3 mg) in a photocatalytic reactor. After adsorption saturation, the bottle was irradiated by an Xe lamp at 400-750 nm (Beijing Perfect Light Technology Co., LTD., Beijing, China). The apparent quantum yield (AQY) of the photocatalyst was measured under the irradiation of a 300 W Xe lamp with band-pass filters (400 nm, 420 nm, 450 nm, 480 nm, 500 nm, 520 nm, 550 nm, 600 nm, 665 nm, 700 nm and 750 nm). The active area of the reactor is about 1

cm². Use PL-MW2000 optical radiometer to take the average value of monochromatic light intensity at three representative points. Therefore, the light intensity is calculated as 10 mW cm⁻². AQY is calculated as follows:

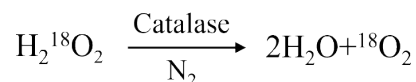
$$\text{AQY} = \frac{\text{Number of production H}_2\text{O}_2 \text{ molecules}}{\text{Number of incident photons}} \times 100$$

$$\text{AQY} = \frac{(M_{\text{H}_2\text{O}_2} \times N_A \times h \times c) \times 2}{S \times P \times T \times \lambda} \times 100$$

Where M is yield of H₂O₂ (mol), N_A is Avogadro constant ($6.02 \times 10^{23} \text{ mol}^{-1}$); h is Planck constant ($6.626 \times 10^{-34} \text{ J}\cdot\text{s}$); c is Speed of light ($3 \times 10^8 \text{ m/s}$); S is Irradiation area (1 cm^2); P is the intensity of irradiation light (10 mW/cm^2); T is the photoreaction time (21600 s); λ is the wavelength of the monochromatic light (nm).

1.9. Isotope labelling experiments

0.03 mg **PDIOH** film floating in 1 mL H₂¹⁸O within a 5 mL volume container for photocatalytic reactions, which was irradiated by Xenon lamp. Following the photosynthetic reaction involving H₂O₂, the reaction mixture was transferred into a 5 mL sealed bottle and subjected to N₂ sparging to eliminate dissolved ¹⁶O₂. The resultant H₂O₂ was then enzymatically decomposed to O₂ using catalase generated in the Nitrogen glove box, denoted as Light-on sample. Control samples (Light-off) were harvested under identical experimental conditions immediately preceding light initiation. The generated O₂ gas was analyzed by a gas chromatography-mass spectrometry (GC-MS, Agilent 7890B-5977B).



1.10. In situ DRIFTS characterization.

In-situ diffuse reflectance infrared Fourier transform spectroscopy (DRIFTS) measurements were performed on a spectrometer (Nicolet iS10 Thermo Scientific, USA). The spectrometer is equipped with a Harrick in-situ cell (including two zinc selenide windows and a quartz window), a high temperature in-situ diffuse reflection accessory and temperature controller, along with a liquid nitrogen cooled mercury cadmium telluride MCT detector. In a typical procedure, the catalyst was placed in a sample cell inside a sealed reaction tank for degassing at 373 K for 3 h. Then, O₂ enters the reaction cell through water vapor for 60 min to achieve an adsorption-desorption equilibrium. Using 365 nm UV lamp ($300 \text{ mW}\cdot\text{cm}^{-1}$) as the light source, the infrared spectrum of different time periods was recorded by in-situ light reaction through the quartz window.

1.11. Femtosecond-transient absorption spectra

Femtosecond transient absorption spectra (TAS) were obtained using a Helios transient absorption spectrometer

coupled with a titanium sapphire laser system (Astrella, Coherent Inc.). Initially, a femtosecond laser amplifier was operated to generate a femtosecond pulsed laser with a repetition frequency of 1 kHz, a maximum laser power of 10 W, a pulse width of 100 fs, and a single-pulse energy of 7 mJ. The output of the femtosecond laser was divided into two beams. A portion of the 800 nm pulsed light is directed into an optical parametric amplifier (OPerA Solo, Coherent) to generate 400/470 nm pump light, while a second portion is transmitted through a delay line to a transient absorption spectrometer (Helios, Ultrafast system). The ultrafast system is focused on a nonlinear crystalline sapphire to produce supercontinuous detection light (430-780 nm). The intensity of the pump laser was regulated by a variable neutral density filter, which was used to excite the sample. The weaker beam was then directed through a motorised optical delay line and focused on a sapphire crystal, resulting in the generation of a supercontinuous white light with a wavelength range of 500-800 nm, which served as the detection light. The optical delay line was employed to vary the relative delay time between the pump light and the detector light by up to 7.6 ns. The temporal resolution of the TAS was determined by the width of the laser pulse and the physical delay line in this study is approximately 140 fs. Consequently, the absorption changes caused by the pump pulse were obtained by recording the spectra with and without the pump pulse. The pulse energy of the excitation light was measured using a PM400 power meter (Thorlabs).

1.12. MD simulations

Molecular dynamics (MD) simulations were performed using the GROMACS package¹⁻³. The system under study consisted of 80 **PDIOH** molecules, 5000 oxygen molecules, and 5000 water molecules. The bi-layer structure of **PDIOH** was derived from the simulated **PDIOH** cif file, based on the refined XRD data, and was used as the initial structure for subsequent MD simulations. The initial configuration of **PDIOH**, along with oxygen and water molecules, was generated using Packmol software⁴, showing **PDIOH** molecules were positioned at the center of the simulation box, oxygen molecules were placed above the **PDIOH** layer, and water molecules occupied the region below the **PDIOH** layer. The system was placed in a simulation box with dimensions of 5.5 nm \times 22 nm \times 5.5 nm.

The force fields for **PDIOH** and oxygen molecules were generated using Sobtop software⁵, employing the Generalized AMBER Force Field (GAFF)⁶ and RESP charges, while the force field for water molecules was defined using the SPC/E model. During the simulation, the position of **PDIOH** remained stable throughout the entire simulation. The system was initially heated to 298.15 K, followed by energy minimization. The MD simulation was then performed in an NVT ensemble for a total simulation time of 5 ns.

In the NVT ensemble, temperature control was maintained using the V-rescale thermostat at 298.15 K. The LINCS algorithm was applied to constrain bond lengths of hydrogen atoms. Electrostatic interactions were evaluated using the Particle-Mesh Ewald (PME) method with a fourth-order interpolation, and a cutoff of 1.0 nm was used for the calculation of short-range van der Waals interactions.

1.13. Electron paramagnetic resonance (EPR) measurements

Spin trapping-EPR tests were recorded using a Bruker EMX plus model spectrometer operating at the X-band frequency (9.4 GHz). 5,5-dimethyl-1-pyrroline N-oxide (DMPO) was used as a spin-trapping reagent to detect $\cdot\text{O}_2^-$. The measurement is as follows: The catalyst (0.03 mg) was floated on a liquid surface containing MeOH (1 mL) and DMPO (0.1 mmol), with oxygen or nitrogen continuously pumped onto the liquid surface. Xenon lamp was used as the light source.

Supplementary Figures

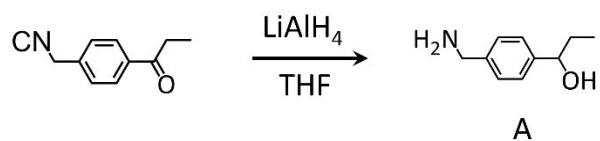


Fig. S1. Synthetic procedure of 1-(4-(aminomethyl)phenyl)propan-1-ol (A).

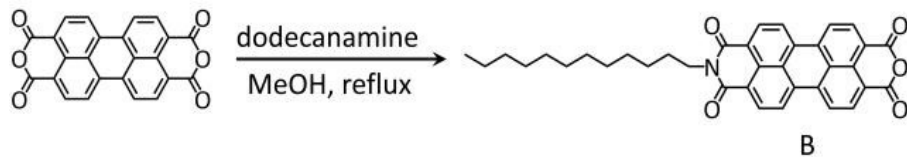


Fig. S2. Synthetic procedure of 9-dodecyl-1H-isochromeno[6',5',4':10,5,6]anthra[2,1,9-def]isoquinoline-1,3,8,10(9H)-tetraone (B).

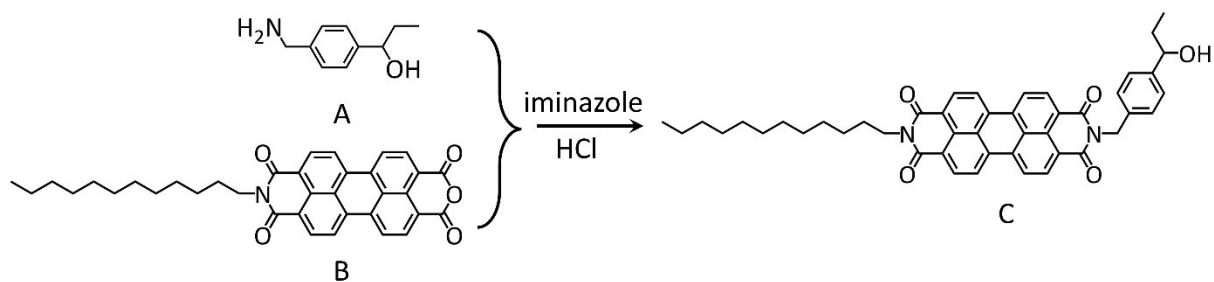


Fig. S3. Synthetic procedure of PDIOH with amphiphilic groups.

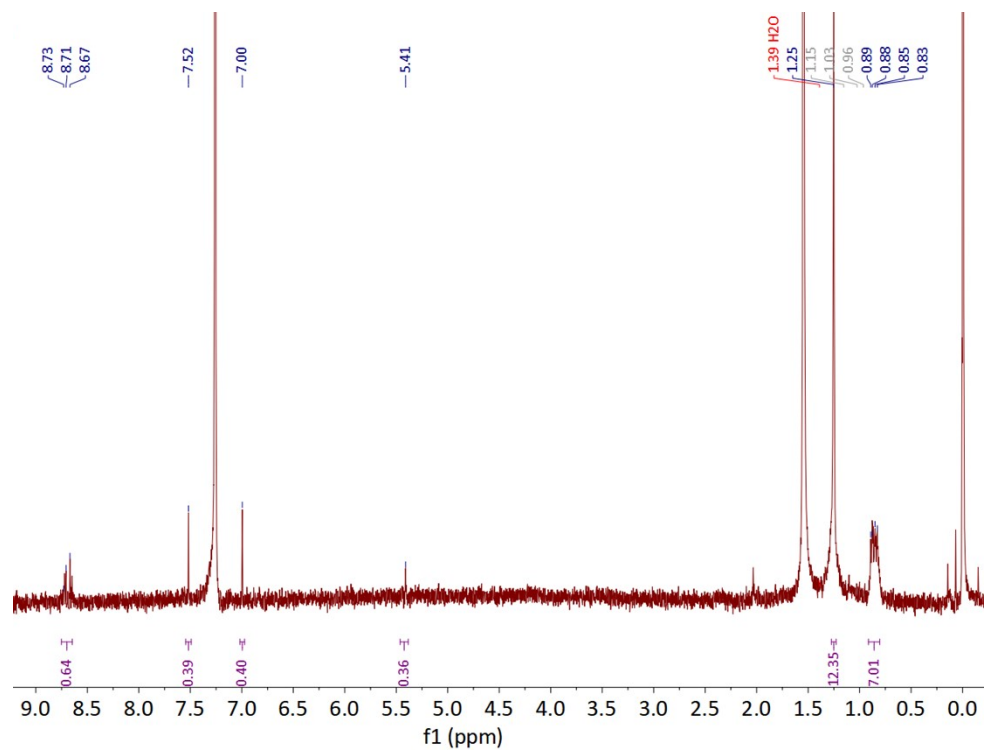


Fig. S4. ¹H NMR of PDIOH.

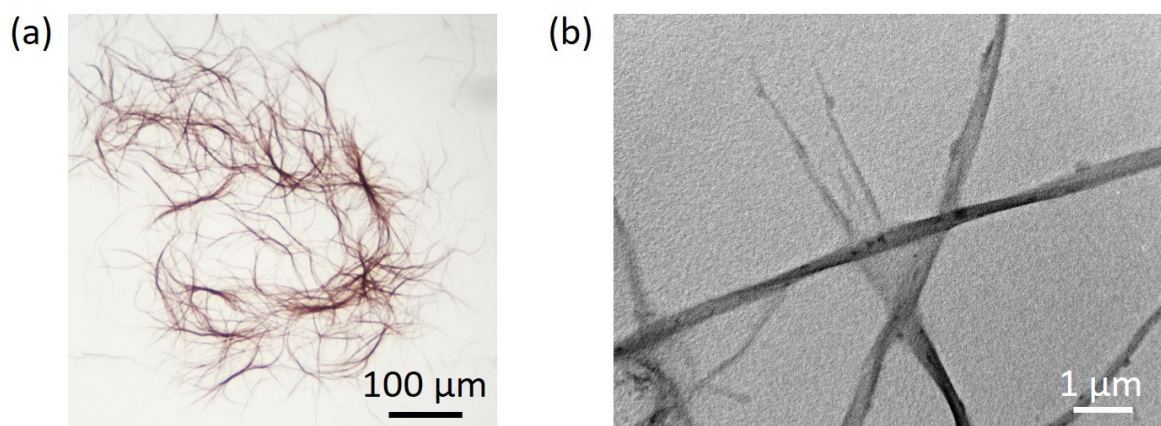


Fig. S5. (a) The photograph and (b) TEM image of self-assembled disordered PDIOH fibers.

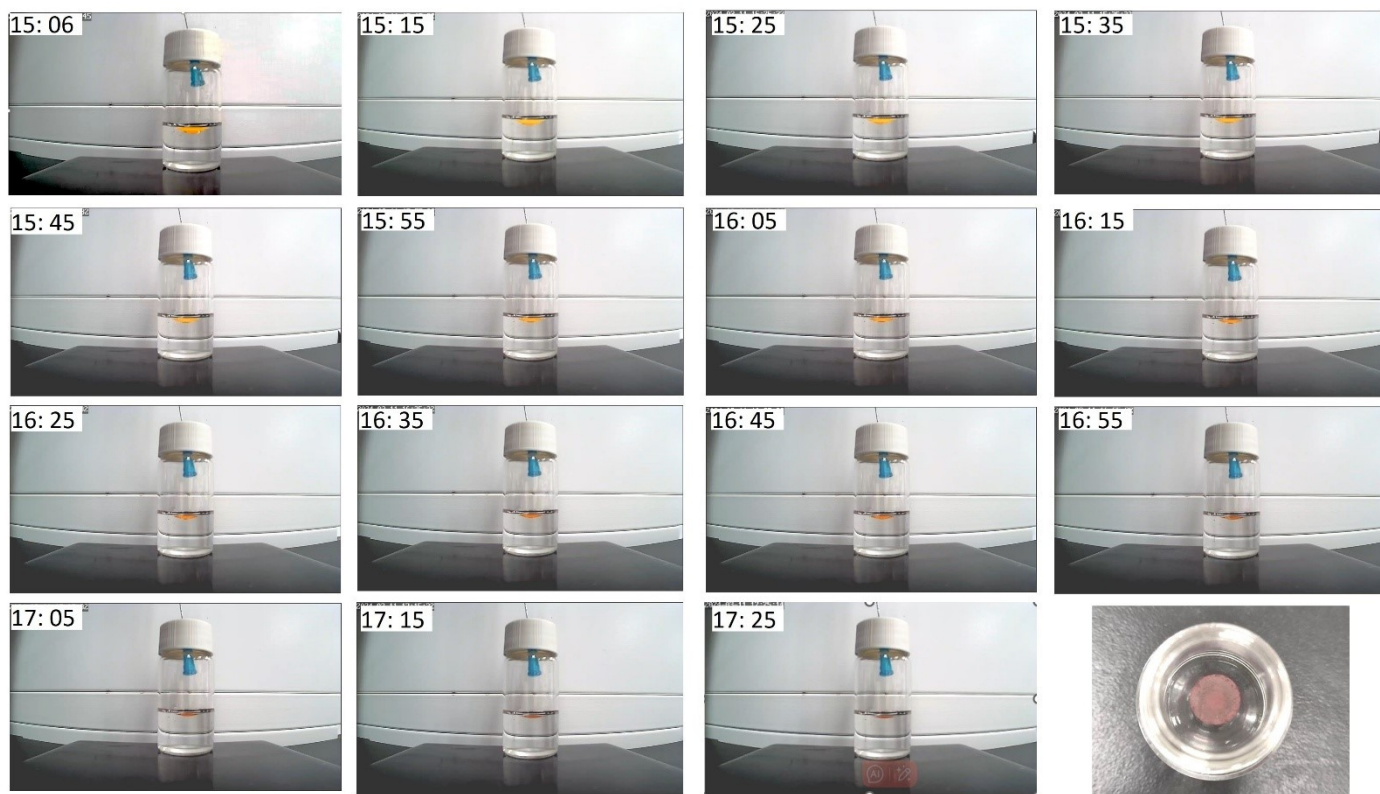


Fig. S6. Photographs depicting the addition of the solution of **PDIOH** (0.1 mg/mL in chloroform) to 10 mL of water in a 20 mL vial under ambient conditions, captured at different time intervals in preparing the 2D hierarchical structure. (15:06 - 17:25).

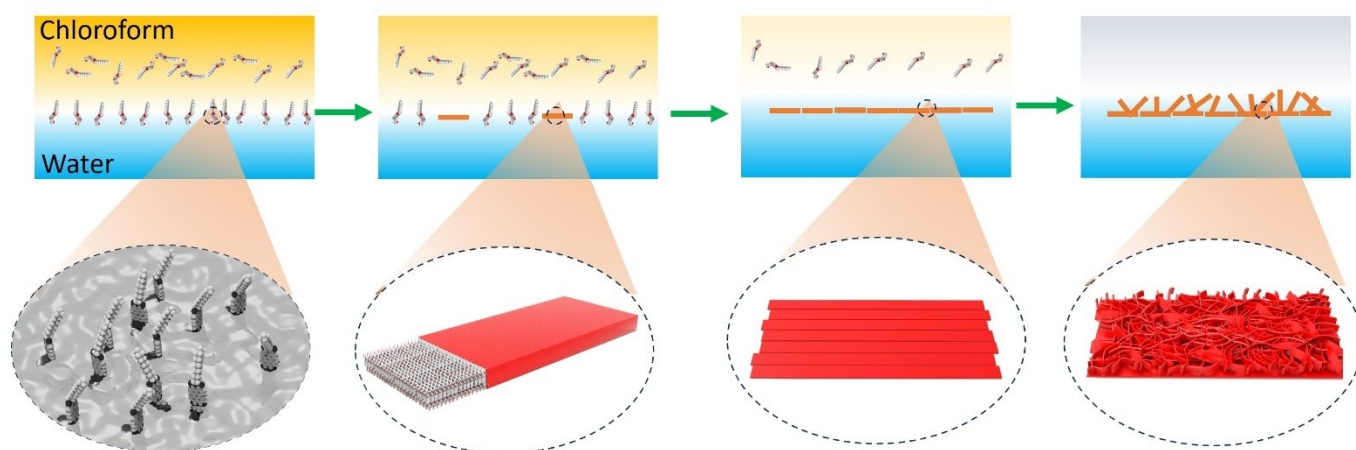


Fig. S7. Schematic diagrams show the self-assembly procedure of the 2D hierarchical **PDIOH** film through interfacial self-assembly at the chloroform-water interface.

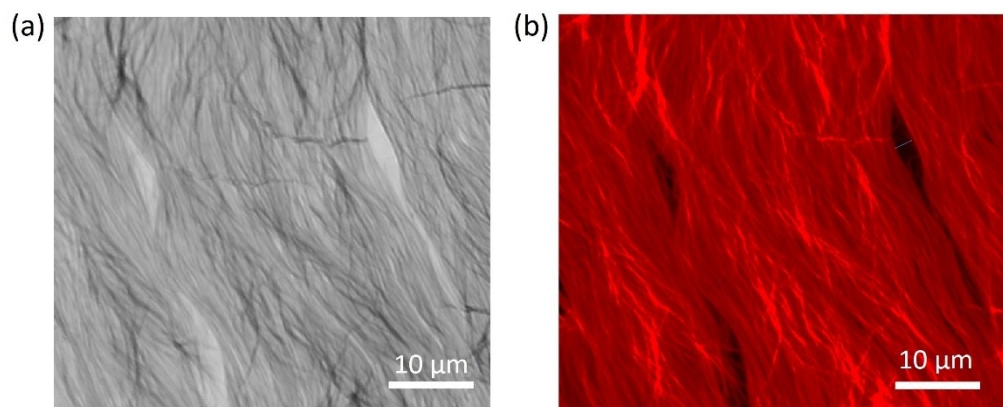


Fig. S8. CLSM images of the **(a)** light field and **(b)** dark field of aligned primary structure **M0** ($\lambda_{\text{ex}} = 405 \text{ nm}$).

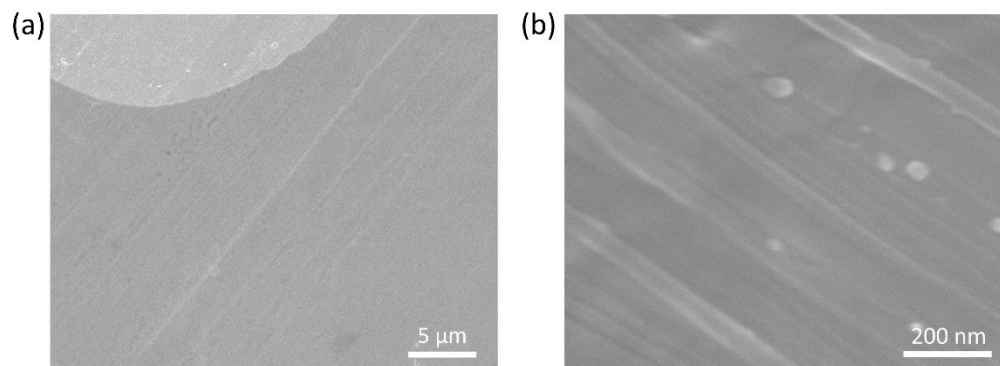


Fig. S9. **(a)** SEM images of highly aligned fibers in the primary structure **M0**. **(b)** Magnified SEM image shows aligned fibers.

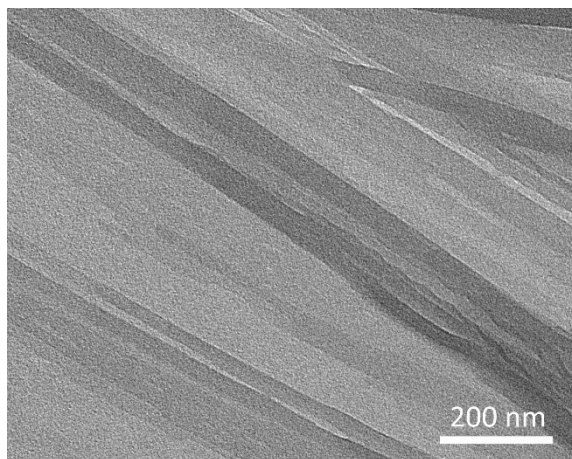


Fig. S10. HRTEM image of highly aligned fibers in primary structure **M0**.

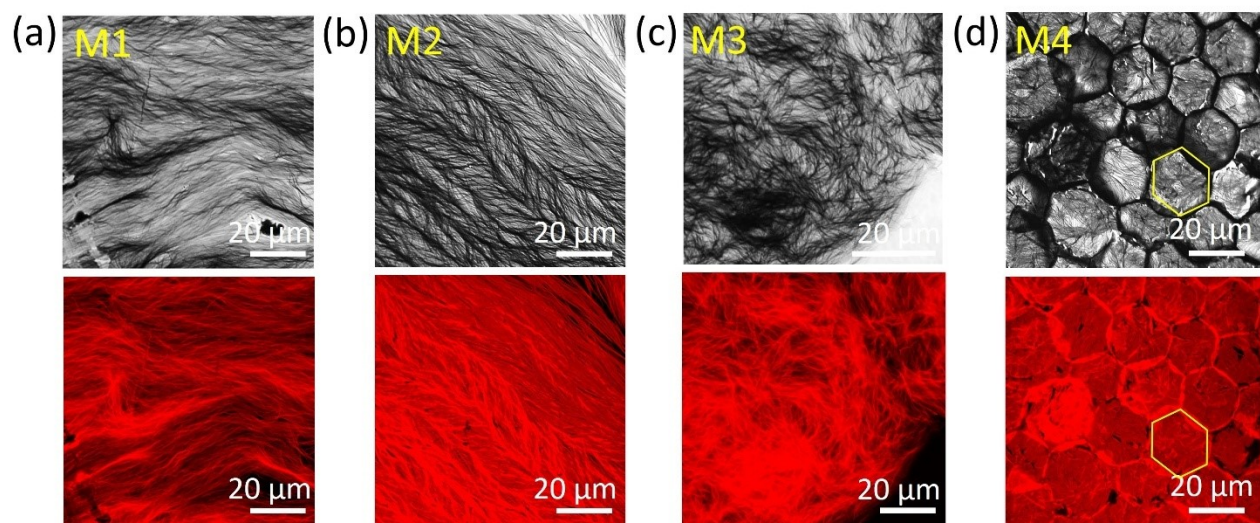


Fig. S11. CLSM images of the light field (top) and dark field (below) to show the morphology evolution of **PDIOH** films (**M1~M4**) by adjusting the feeding amount of **PDIOH** chloroform solution (120 μL , 150 μL , 200 μL , and 250 μL) during the self-assembly ($\lambda_{\text{ex}} = 405 \text{ nm}$).

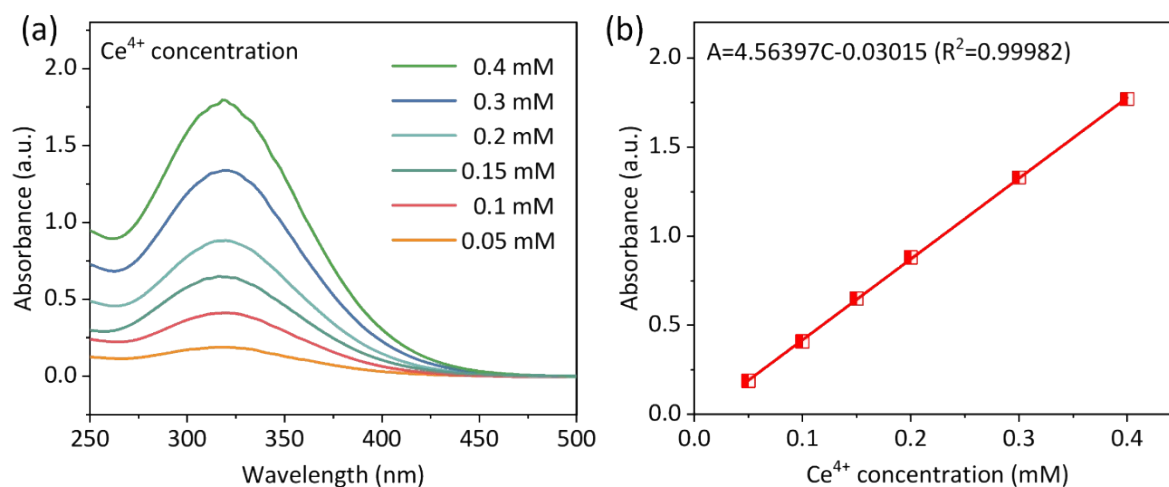


Fig. S12. (a) The change of absorption intensity at 316 nm with several known concentrations of $\text{Ce}(\text{SO}_4)_2$ solution measured by UV-vis spectrometer; (b) The standard curve of H_2O_2 concentration-absorbance by $\text{Ce}^{3+/4+}$ back-titration.

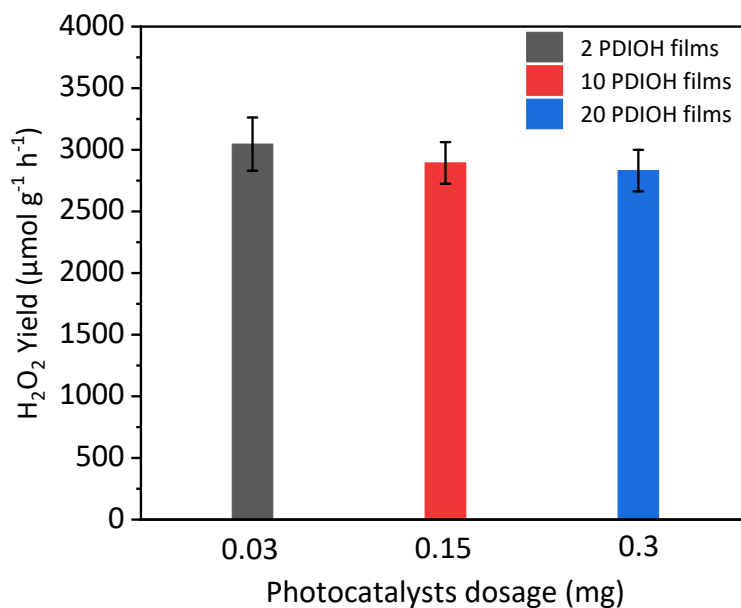


Fig. S13. H_2O_2 yield by **PDIOH** film with different dosage in ultrapure water. The H_2O_2 yield can reach $3046.15 \mu\text{mol g}^{-1} \text{h}^{-1}$, $2894.12 \mu\text{mol g}^{-1} \text{h}^{-1}$ and $2831.68 \mu\text{mol g}^{-1} \text{h}^{-1}$ with the addition of 0.03 mg, 0.15 mg and 0.3 mg **PDIOH** films in 20 mL ultrapure water, respectively. Error bars (in standard deviation) were obtained by statistically repeating identical experimental results three times. Conditions: Xenon lamp ($1000 \text{ mW} \cdot \text{cm}^{-2}$), **PDIOH** films floated in ultrapure water (20 mL).

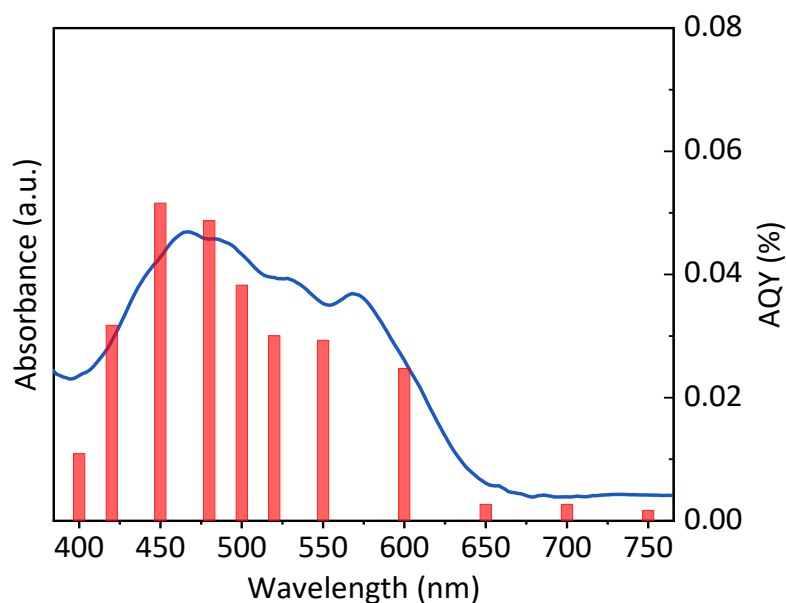


Fig. S14. The wavelength-dependent apparent quantum yield (AQY) of the **PDIOH** film in the photocatalytic H_2O_2 production, 400 nm, 420 nm, 450 nm, 480 nm, 500 nm, 520 nm, 550 nm, 600 nm, 650 nm, 700 nm and 750 nm. Conditions: Catalyst dosage (0.3 mg), Light intensity ($10 \text{ mW} \cdot \text{cm}^{-2}$), **PDIOH** films floated in ultrapure water (20 mL).

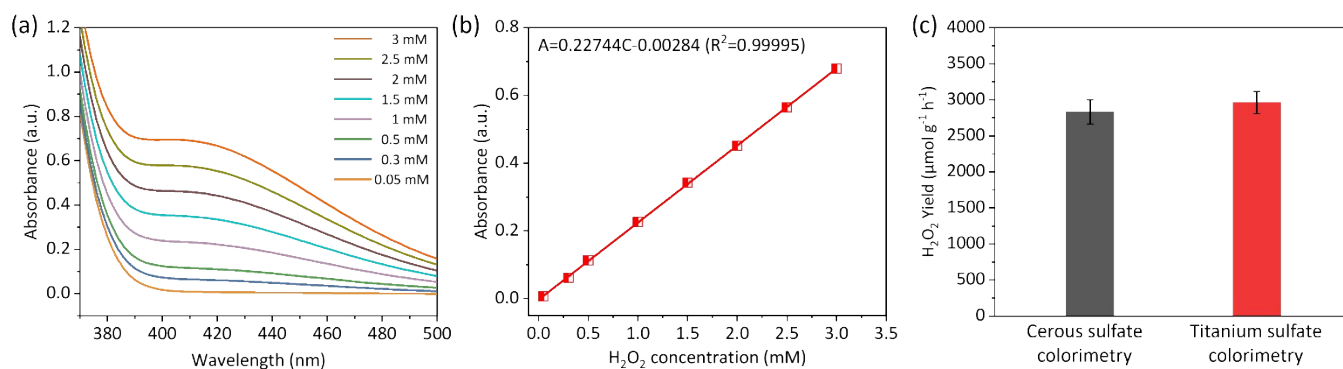


Fig. S15. (a) A known concentration of H_2O_2 solution was added to titanium sulfate solution, and the change of absorption intensity at 416 nm was measured by UV-vis spectrometer.; (b) The standard curve of H_2O_2 concentration-absorbance. (c) Comparing the H_2O_2 synthesis performance on **PDIOH** films using cerium ion method and titanium sulfate method. Conditions: Xenon lamp ($1000 \text{ mW} \cdot \text{cm}^{-2}$), 0.3 mg catalyst (20 **PDIOH** films) floated in ultrapure water (20 mL). Error bars (in standard deviation) were obtained by statistically repeating identical experimental results three times.

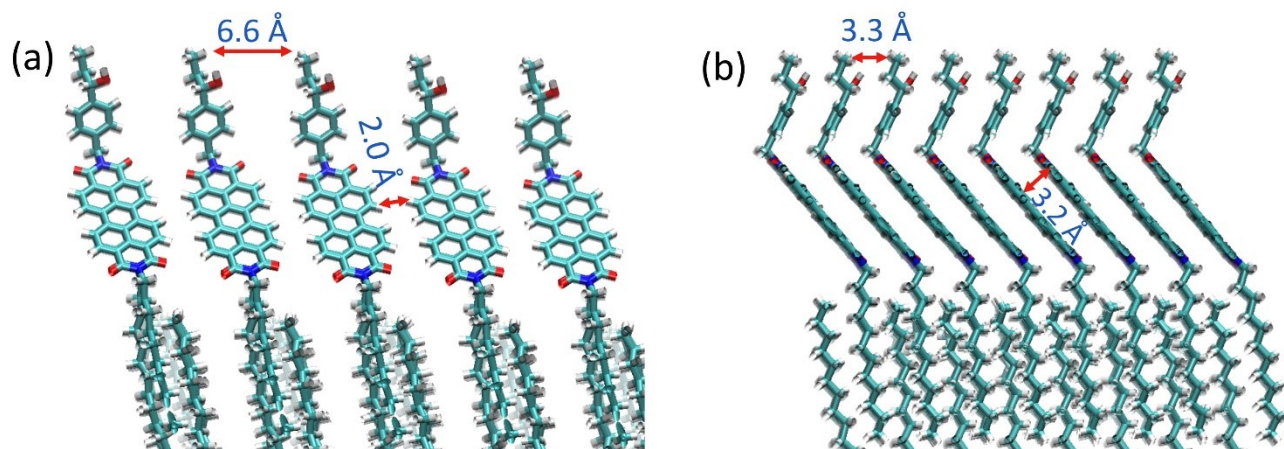


Fig. S16. The intermolecular distance in **PDIOH** fibers in (a) front view and (b) side view.

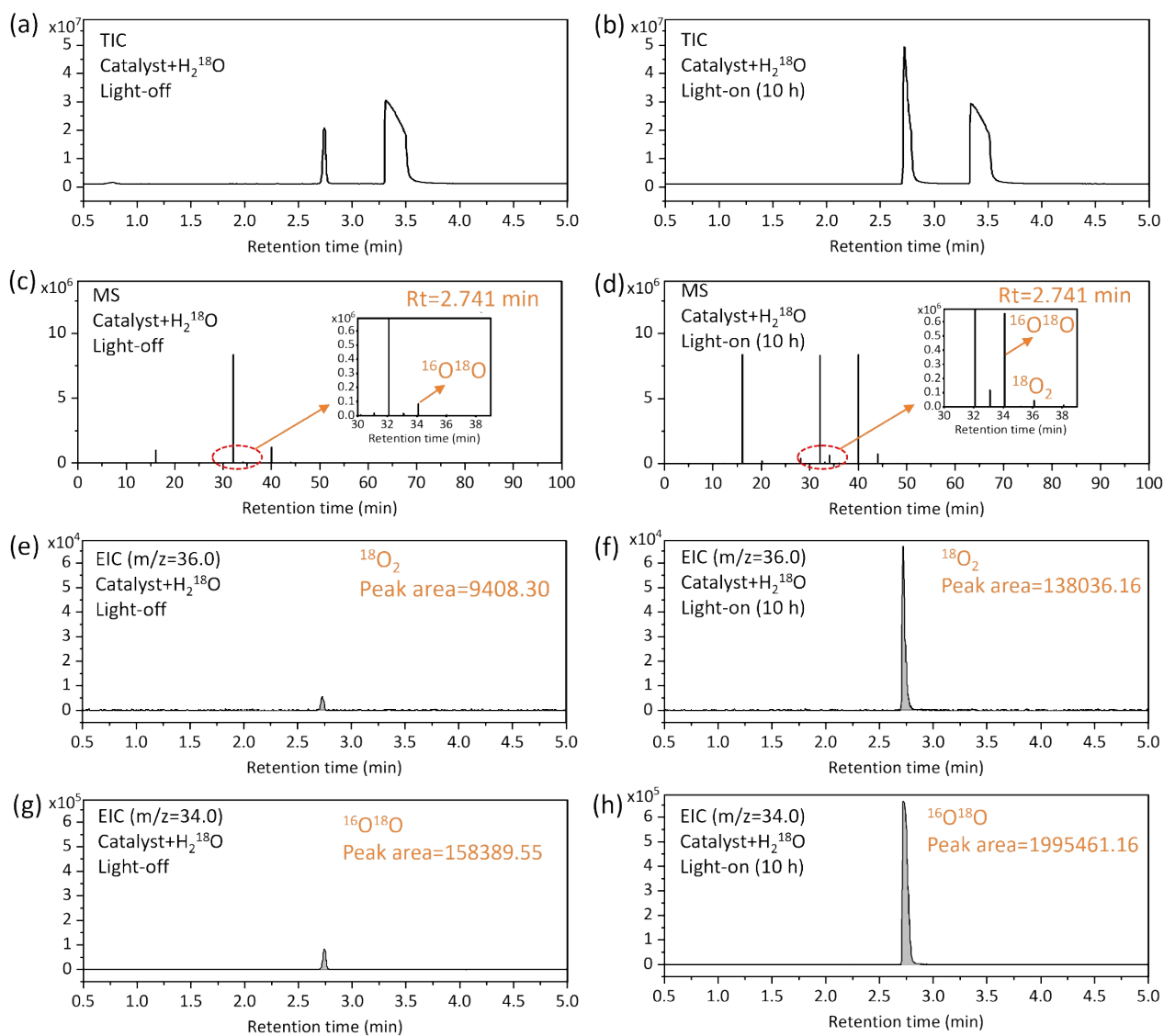


Fig. S17. GC-MS analysis (using an Agilent CP-7533 5A column at 70 eV) was employed for isotope-tracing experiments involving $^{18}\text{O}_2$ and $^{16}\text{O}^{18}\text{O}$. In these experiments, H_2^{18}O was oxidized to $\text{H}_2^{18}\text{O}_2$ via catalysis, followed by enzymatic decomposition using catalase (catalyst/ H_2^{18}O = 0.03 mg/1 mL): the TIC of 1 mL products generated by (a) light-off and (b) light-on for 10 h, the corresponding MS spectra (RT=2.741 min) of 1 mL products generated by (a) light-off and (b) light-on for 10 h (inset shows the 25-fold amplification of y-axis scale), EIC (m/z =36.0) of 1 mL products generated by (c) light-off and (f) light-on for 10 h, EIC (m/z =34.0) of 1 mL products generated by (e) light-off and (f) light-on for 10 h.

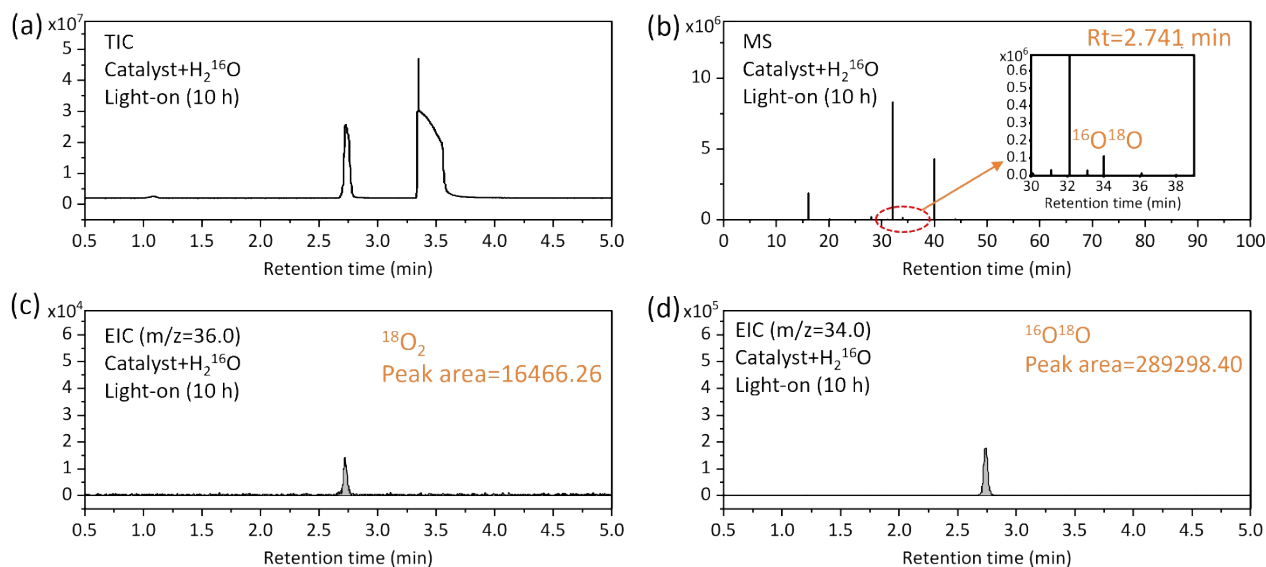


Fig. S18. GC-MS analysis (using an Agilent CP-7533 5A column at 70 eV) was employed for isotope-tracing experiments involving ^{18}O and $^{16}\text{O}^{18}\text{O}$. In this experiments, H_2^{16}O was oxidized to $\text{H}_2^{16}\text{O}_2$ via catalysis, followed by enzymatic decomposition using catalase (catalyst/ H_2^{16}O = 0.03 mg/1 mL): (a) the TIC of 1 mL products generated by light-on for 10 h, (b) the corresponding MS spectra (RT=2.741 min) of 1 mL products generated by light-on for 10 h (inset shows the 25-fold amplification of y-axis scale), (c) EIC (m/z =36.0) of 1 mL products generated by light-on for 10 h, (d) EIC (m/z =34.0) of 1 mL products generated by light-on for 10 h.

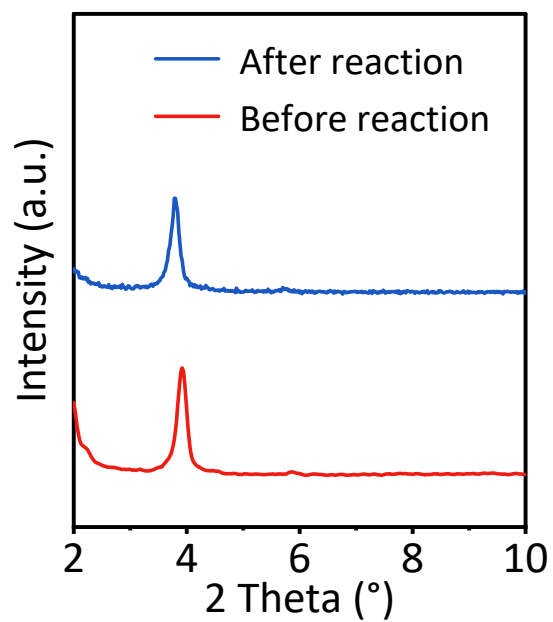


Fig. S19. XRD spectra of **M2** before and after 20 hours of continuous reaction operation.

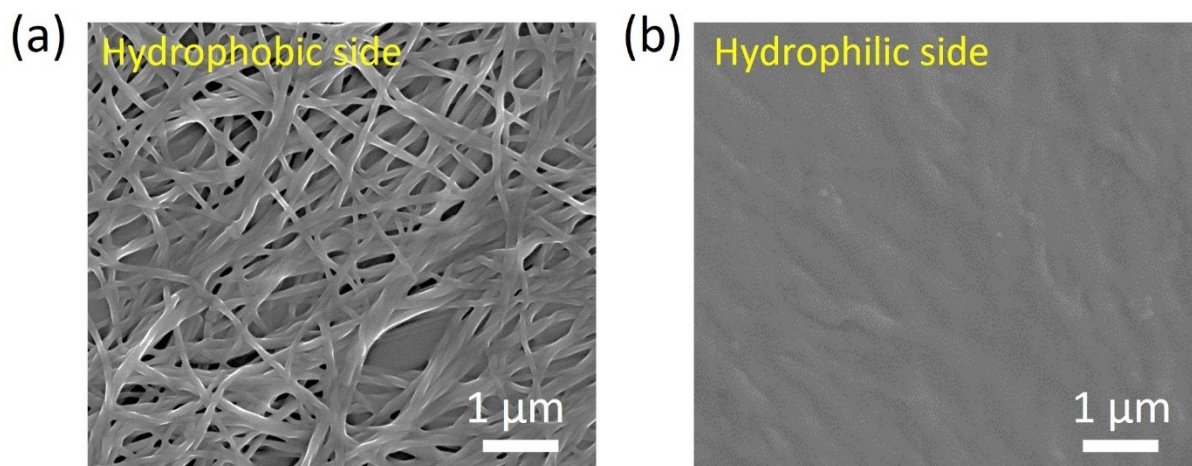


Fig. S20. The SEM images of hydrophobic and hydrophilic sides of **M2** after 20 hours of continuous reaction operation.

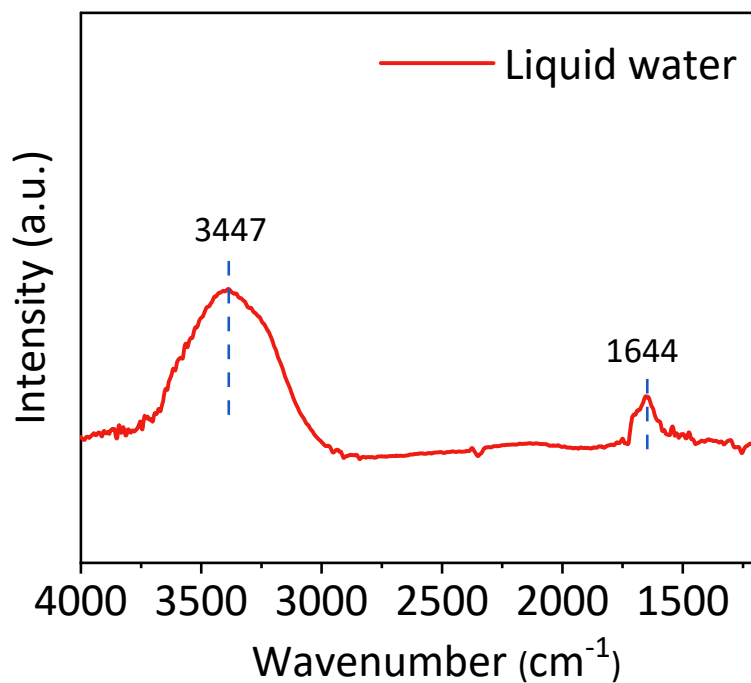


Fig. S21. Image of FTIR spectra of liquid water. (3447 cm⁻¹: O-H stretching; 1644 cm⁻¹: H-O-H bending).

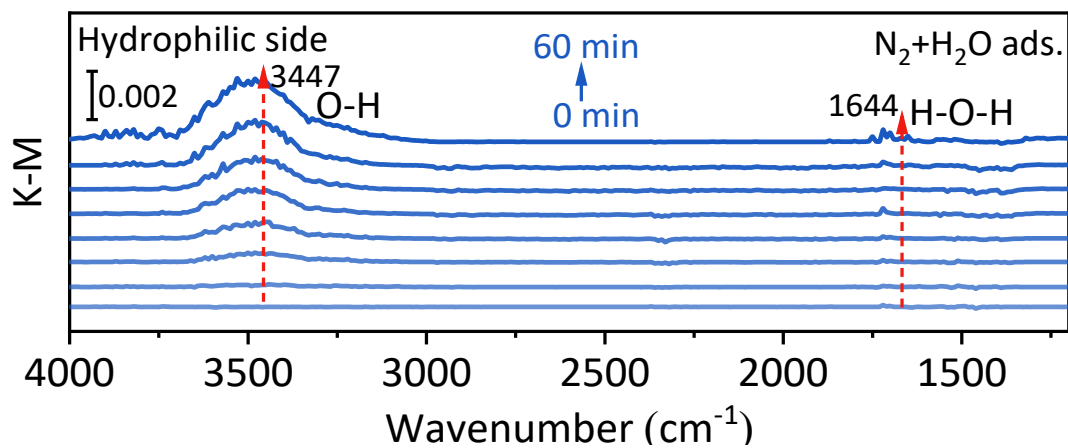


Fig. S22. In situ DRIFTS time spectra of continuous H₂O adsorption on the hydrophilic side of **PDIOH** films (**M2**).

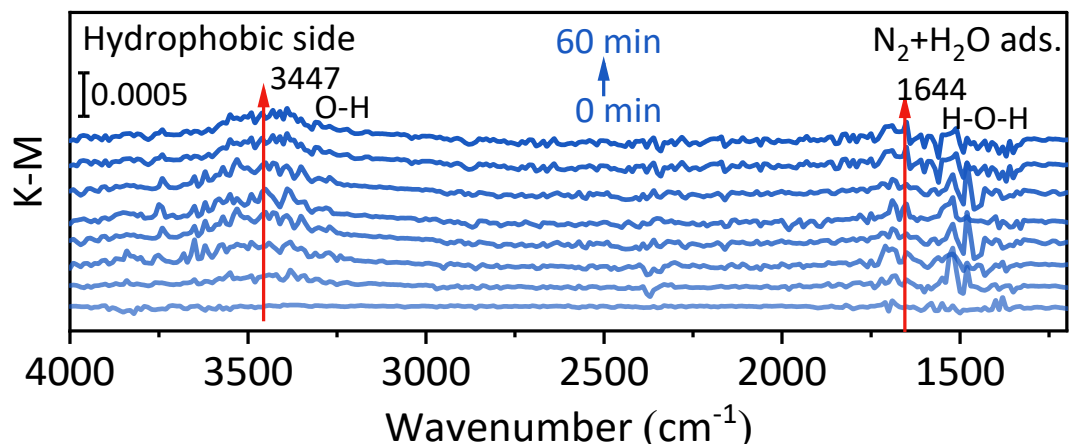


Fig. S23. In situ DRIFTS time spectra of continuous H₂O adsorption on the hydrophobic side of **PDIOH** film (**M2**).

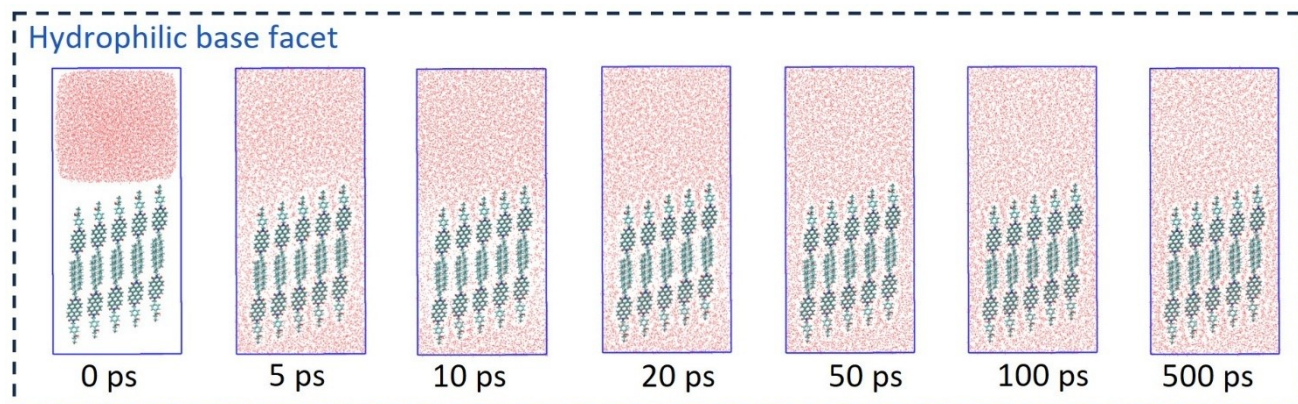


Fig. S24. MD time-slides of the hydrophilic base facet confronting O₂ molecules.

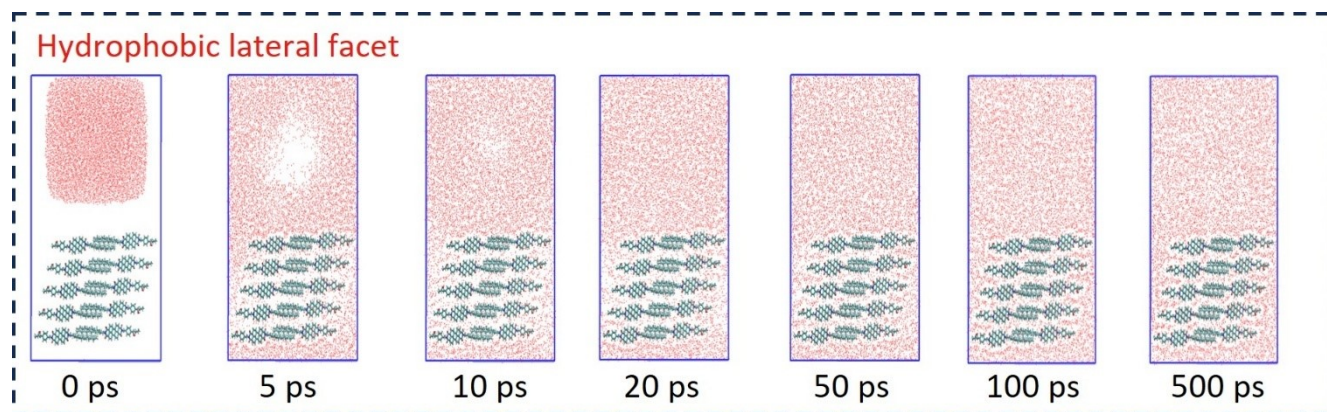


Fig. S25. MD time-slides of the hydrophobic lateral facet confronting O_2 molecules.

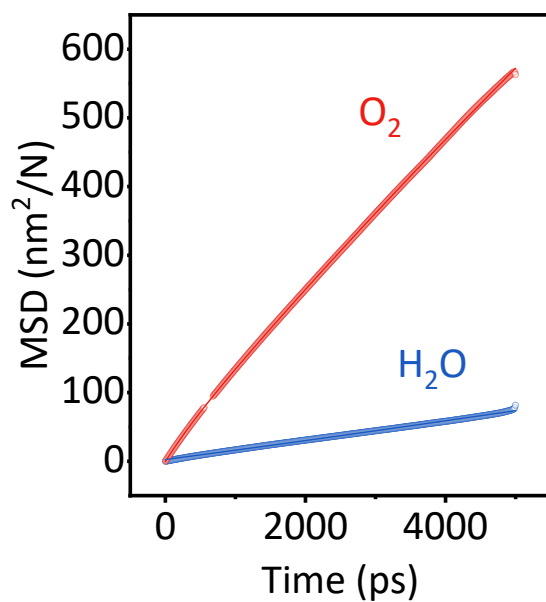


Fig. S26. Time-profiles of O_2 and H_2O accumulated at the triphasic interface.

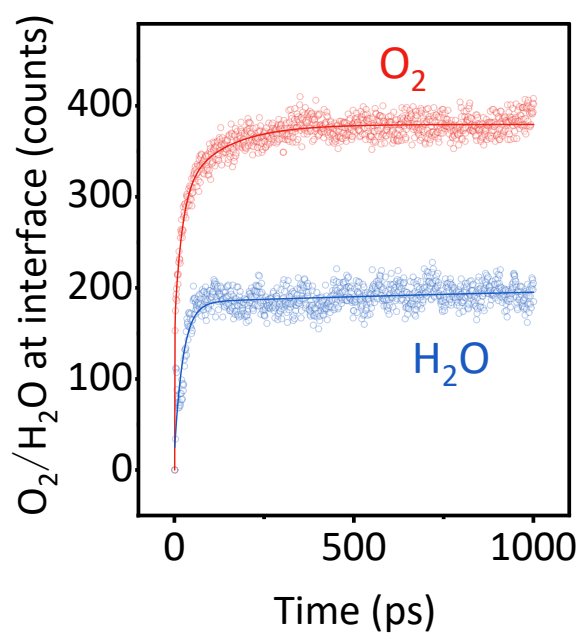


Fig. S27. Mean square displacement for O_2 and H_2O diffusion within the **PDIOH** film.

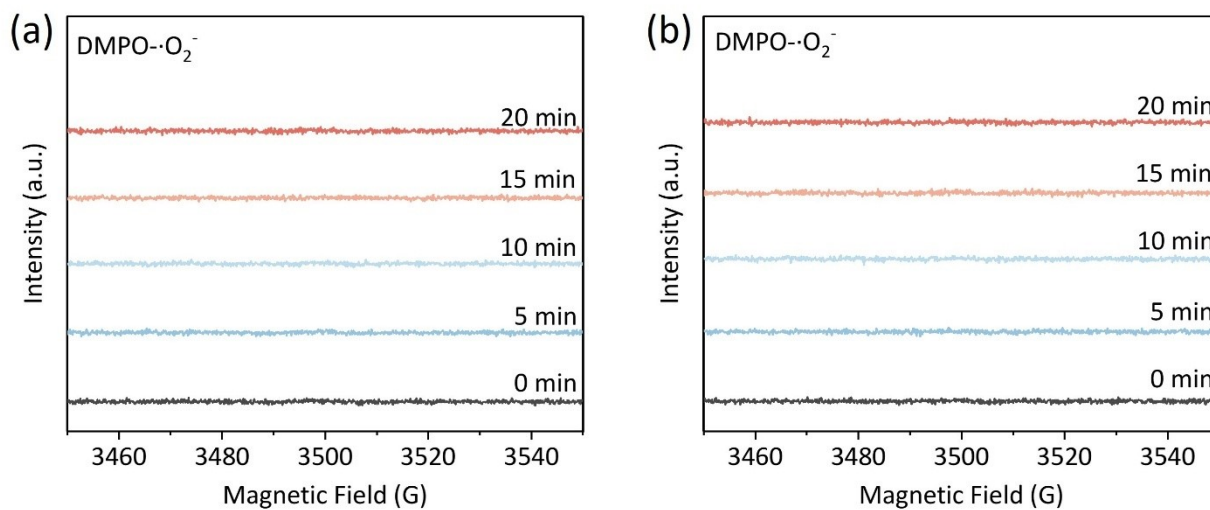


Fig. S28. EPR spectra of (a) without **PDIOH** film in O_2 atmosphere and (b) **PDIOH** film in N_2 atmosphere under Xenon lamp irradiation, using DMPO as the spin-trapping chemical in MeOH solution.

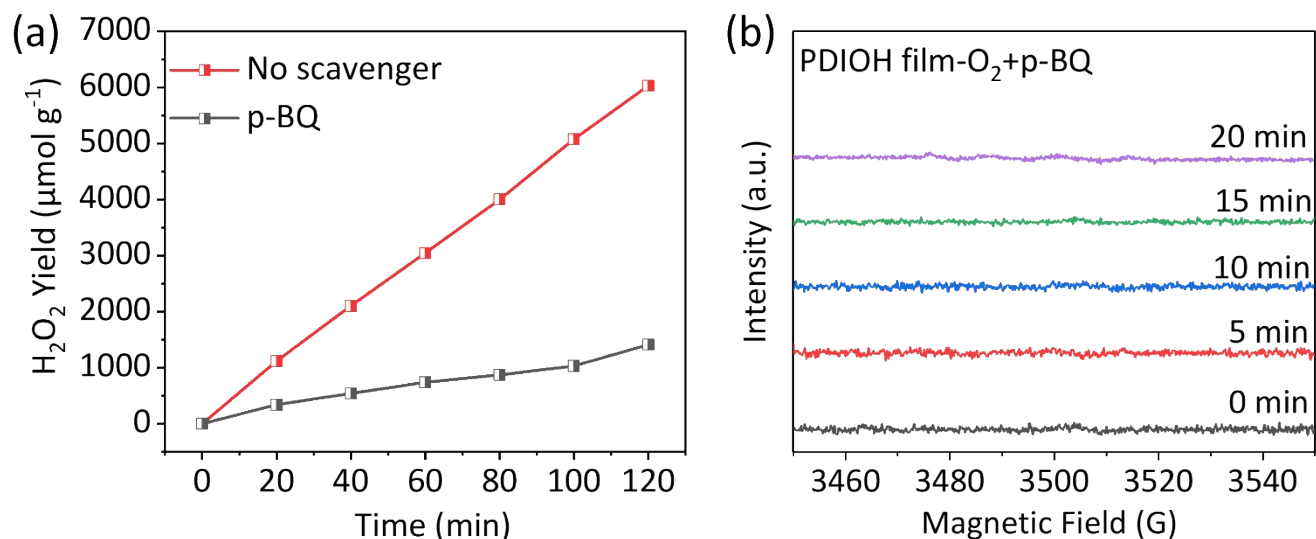


Fig. S29. Quenching experiments for H_2O_2 photosynthesis. Experimental conditions: (xenon lamp, light intensity: 1000 mW cm^{-2}), volume (10 mL), photocatalyst (0.03 mg), $[\text{p-BQ}]_0 = 0.3 \text{ mM}$. (b) EPR spectra of **PDIOH** film in O_2 atmosphere under Xenon lamp irradiation after the addition of p-BQ, using DMPO as the spin-trapping chemical in MeOH solution.

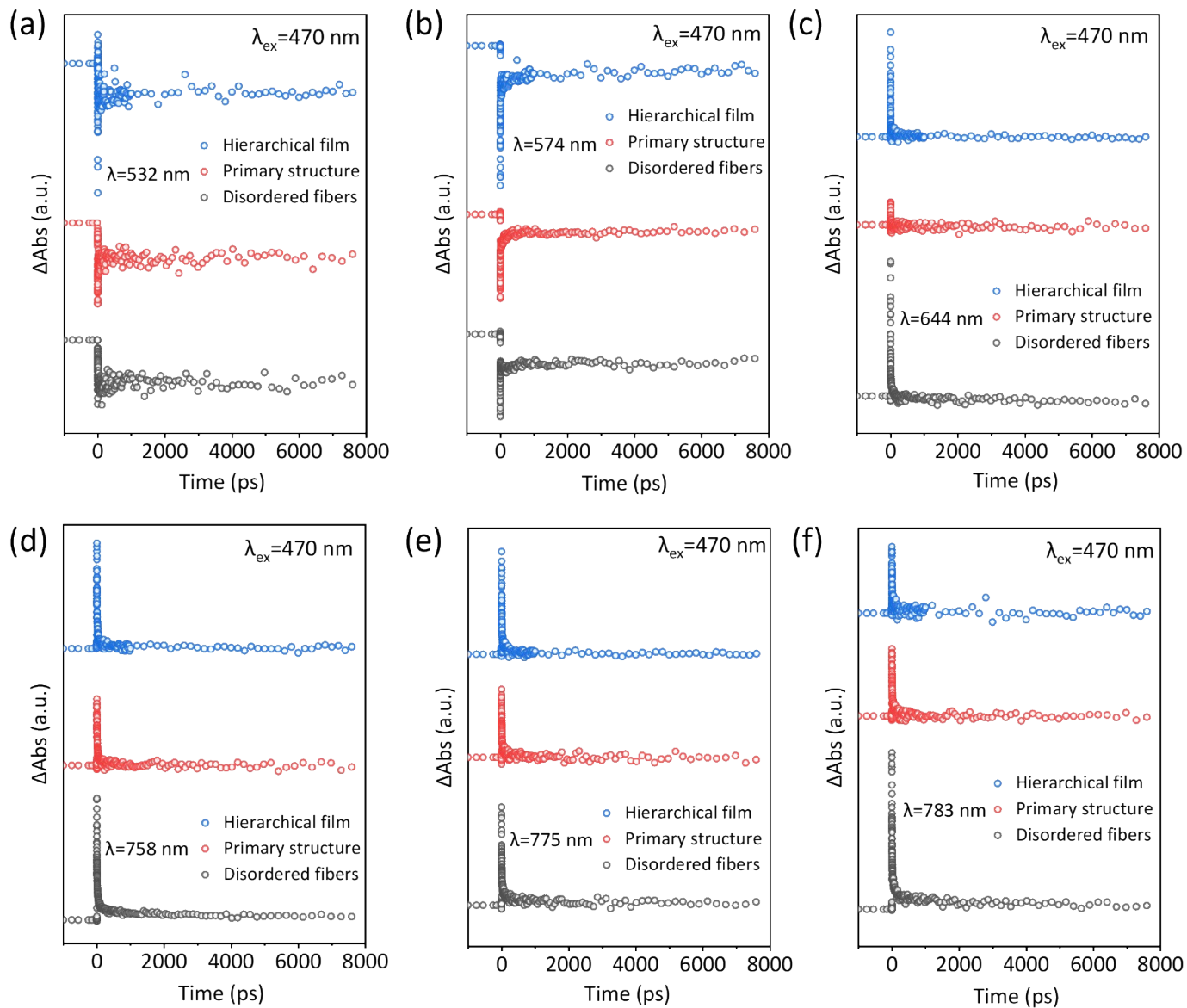


Fig. S30. Time-profiles of fiber-fiber transition bleaching and ESA at 532 nm, 574 nm, 644 nm, 758 nm, 775 nm and 783 nm, respectively, on Disordered fibers, Primary structure and Hierarchical film, ($\lambda_{\text{ex}} = 470$ nm).

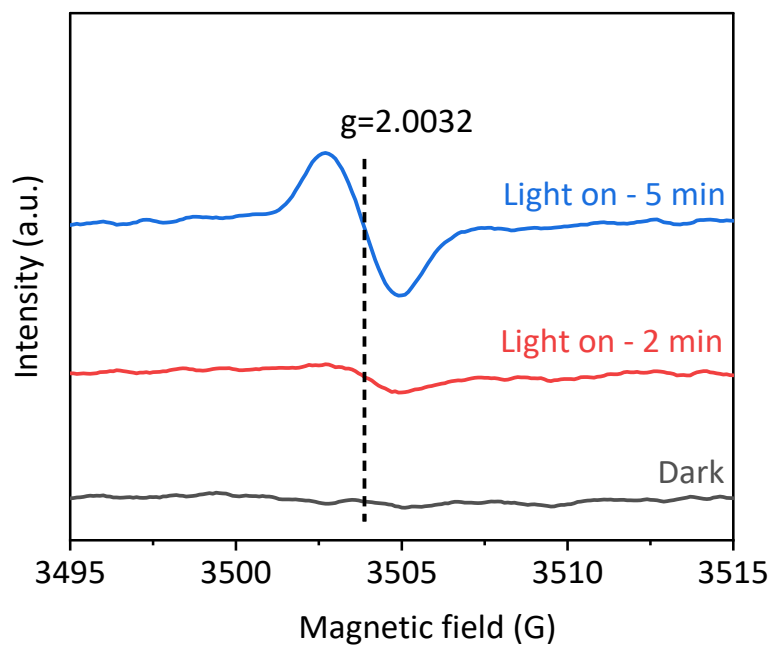


Fig. S31. EPR spectra of **PDIOH** film under different light exposure times. Conditions: The **PDIOH** film was dispersed in 100 μL of methanol. Testing was performed under irradiation with 470 nm monochromatic light in an ambient air atmosphere.

Table S1. Wavelength-dependent AQYs and corresponding H₂O₂ production amount on **PDIOH** film.

Wavelength (nm)	H ₂ O ₂ evolution (μ mol)	Light intensity (mW cm ⁻²)	Irradiation area (cm ²)	Irradiation time (h)	AQY (%)
400	23.6	10.0	1.0	6	0.0109
420	24.03	10.0	1.0	6	0.0317
450	41.91	10.0	1.0	6	0.0516
480	42.19	10.0	1.0	6	0.0487
500	34.56	10.0	1.0	6	0.0383
520	28.16	10.0	1.0	6	0.03
550	29.09	10.0	1.0	6	0.0293
600	26.75	10.0	1.0	6	0.0247
650	3.17	10.0	1.0	6	0.0027
700	3.41	10.0	1.0	6	0.0027
750	2.30	10.0	1.0	6	0.0017

References

- 1 D. Van Der Spoel, E. Lindahl, B. Hess, G. Groenhof, A. E. Mark, H. Berendsen, *J. Comput. Chem.* 2005, **26**, 1701-1718.
- 2 M. J. Abraham, T. Murtola, R. Schulz, S. Páll, J. C. Smith, B. Hess, E. J. S. Lindahl, *SoftwareX* 2015, **1**, 19-25.
- 3 B. Hess, C. Kutzner, D. Van Der Spoel, E. Lindahl, *J. Comput. Chem.* 2008, **4**, 435-447.
- 4 L. Martínez, R. Andrade, E. G. Birgin, J. Martínez, *J. Comput. Chem.* 2009, **30**, 2157-2164.
- 5 T. S. v. Lu, V. J. S. Sobtop, 2022.
- 6 J. Wang, R. M. Wolf, J. W. Caldwell, P. A. Kollman, D. Case, *J. Comput. Chem.* 2004, **25**, 1157-1174.